



Research article

HBO1/KAT7/MYST2 HAT complex regulates human adenovirus replicative cycle

Heba Kamel^a, Varsha Shete^a, Sayikrushna Gadamsetty^{a, b}, Drayson Graves^b,
Scott Bachus^b, Nikolas Akkerman^b, Peter Pelka^{b,*,1}, Bayar Thimmapaya^{a,**,1}

^a Microbiology and Immunology Department, Fienberg School of Medicine, Northwestern University, Chicago, USA

^b Department of Microbiology, and Department of Medical Microbiology and Infectious Diseases, University of Manitoba, Winnipeg, Canada

ARTICLE INFO

Keywords:

Adenovirus type 5
E1A
HBO1
Viral replication
HAT
Chromatin

ABSTRACT

Human adenoviruses (HAdV) belong to a small DNA tumor virus family that continues as valuable models in understanding the viral strategies of usurping cell growth regulation. A number of HAdV type 2/5 early viral gene products interact with a variety of cellular proteins to build a conducive environment that promotes viral replication. Here we show that HBO1 (Histone Acetyltransferase Binding to ORC1), a member of the MYST histone acetyltransferase (HAT) complex (also known as KAT7 and MYST2) that acetylates most of the histone H3 lysine 14, is essential for HAdV5 growth. HBO1/MYST2/KAT7 HAT complexes are critical for a variety of cellular processes including control of cell proliferation. In HBO1 downregulated human cells, HAdV5 infection results in reduced expression of E1A and other viral early genes, virus growth is also reduced significantly. Importantly, HBO1 downregulation reduced H3 lysine 14 acetylation at viral promoters during productive infection, likely driving reduced viral gene expression. HBO1 was also associated with viral promoters during infection and co-localized with viral replication centers in the nuclei of infected cells. In transiently transfected cells, overexpression of E1A along with HBO1 stimulated histone acetyltransferase activity of HBO1. E1A also co-immunoprecipitated with HBO1 in transiently transfected cells. In summary, our results demonstrate that HAdV recruits the HBO1 HAT complex to aid in viral replication.

1. Introduction

HAdV type 2/5, which replicate in cell nuclei, belong to the small DNA tumor virus family [1]. HAdV is a time-honored model system used to study virus-host cell interactions as well as viral oncogenesis. HAdV5 Early protein 1A (E1A) is a prototype small DNA virus oncoprotein [2]. E1A cooperates with other viral or cellular oncoproteins to drive cellular transformation and can independently induce cellular DNA replication in growth arrested cells [2]. E1A targets a number of different chromatin remodeling factors including p300/CBP [3], GCN5 [4], and pCAF [5]. Known histone acetyl transferases (HATs) belong to at least five different families: KAT3 [6], GCN5/pCAF [7], Rtt109 [8], HAT1 [9] and MYST [10]. Histone Acetyltransferase Binding To ORC1 (HBO1, also known as MYST2 and KAT7 and henceforth referred to as HBO1) is a member of the MYST complex [11]. HBO1 functions as the core catalytic subunit that

* Corresponding author.

** Corresponding author.

E-mail addresses: peter.pelka@umanitoba.ca (P. Pelka), b-thimmapaya@northwestern.edu (B. Thimmapaya).

¹ Equal senior coauthors.

contains a domain known as MYST within its C-terminal region [11]. The MYST domain is responsible for HBO1 HAT activity. HBO1 complexes are multimeric and normally consist of two native subunits (ING4 or ING5 and MEAF6) and two types of cofactors as chromatin readers (BRPF1/2/3 and JADE1/2/3)^{12,13}. The potential choices of different subunits to form the HBO1 complexes provide a regulatory switch to potentiate its activity between histone H4 and H3 tails [11]. Acetylation of histone H4 by HBO1 has been shown to be essential for DNA replication licensing [13–15], while acetylation of histone H3 plays an important role in gene expression [12, 16].

E1A, the first viral protein expressed after infection of human cells with HAdV [17,18], is responsible for a variety of functions including activation of all viral promoters and reprogramming of the infected cell in order to facilitate viral reproduction [2]. E1A functions by altering the activity of other cellular and viral factors to advance the viral replication program and enable progeny viruses to be produced. One way in which E1A achieves these goals is via altering gene expression. To this end, E1A interacts with many components of the cellular transcriptional machinery including chromatin remodeling factors and transcriptional regulators [2,19,20]. One such interaction occurs between the HAT p300/CBP and E1A, which is essential for E1A-mediated transactivation of viral promoters in a Conserved Region (CR) 3-mediated fashion [3]. The mechanism of how this drives gene expression is still unclear, but one possibility is that E1A brings these chromatin remodelers to the promoter to allow gene expression to commence. Indeed, E1A can

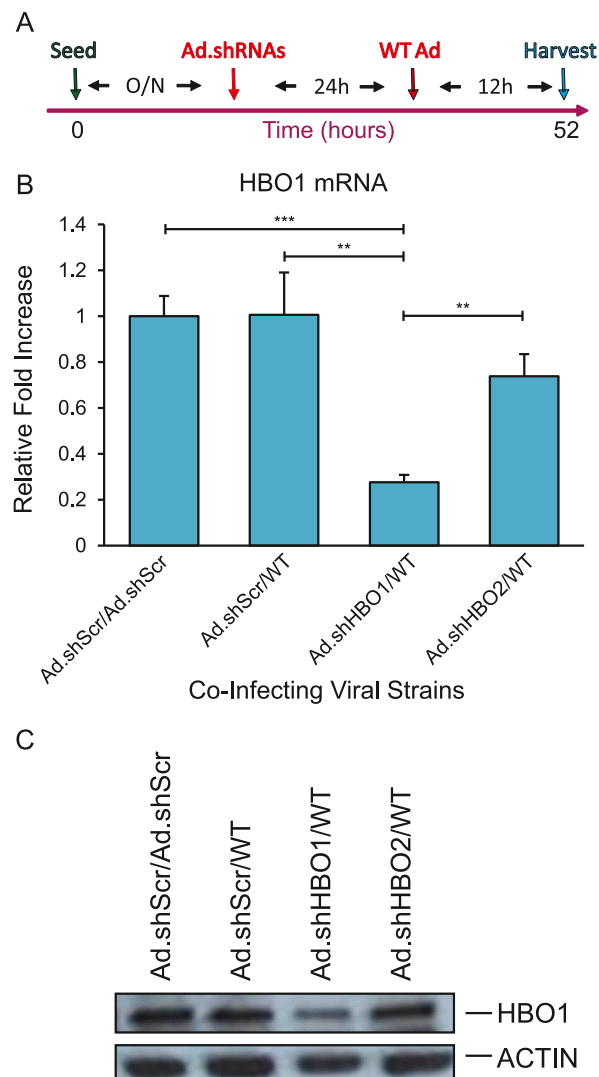


Fig. 1. HBO1 RNA and protein levels are downregulated in MCF10A cells infected with Ad.shHBO1. A. Schematic showing the time course of virus infections. O/N - overnight. B. RT-qPCR data of HBO1 RNA levels in cells infected, using the infection protocol shown in panel A, with the indicated viruses. Fold change is tabulated using the $\Delta\Delta Ct$ method versus cells infected only with Ad.shScr control virus. Ad.shScr - expresses negative control scrambled shRNA targeting eGFP, others express shRNA targeting human HBO1. Error bars represent standard deviation with * - $p \leq 0.05$, ** - $p \leq 0.01$, *** - $p \leq 0.001$; $n = 3$. C. Representative Western blot showing decreased levels of HBO1 protein in cells infected with Ad.shHBO1. Ad.shScr vector expresses scrambled sequences targeting eGFP. Ad.shHBO1 and Ad.shHBO2 vectors target different regions of human HBO1 mRNAs. Uncropped blots are shown in supplemental figures.

associate with cellular promoter-bound transcriptional regulators and alter their function directly, such as by turning a repressive E2F complex into an activating one [21]. Our laboratories have been interested in the epigenetic regulation of HAAdVs. For example, we showed earlier that p300 controls E1A transcription by inducing c-Myc and also at the promoter level by epigenetic modifications [22–24].

In the present study, we report our initial findings that HBO1 protein is essential for HAAdV replication. Virus yield is significantly reduced in human cells when HBO1 is knocked down by shRNAs. Importantly, HBO1 knockdown significantly reduced histone H3 lysine (K) 14 acetylation at viral promoters during productive infection, significantly reducing viral gene expression. HBO1 was also associated with viral promoters during infection and co-localized with viral replication centers in the nuclei of infected cells. To our knowledge, this is the first report of the involvement of the MYST2 complex in the replication of a small DNA tumor virus.

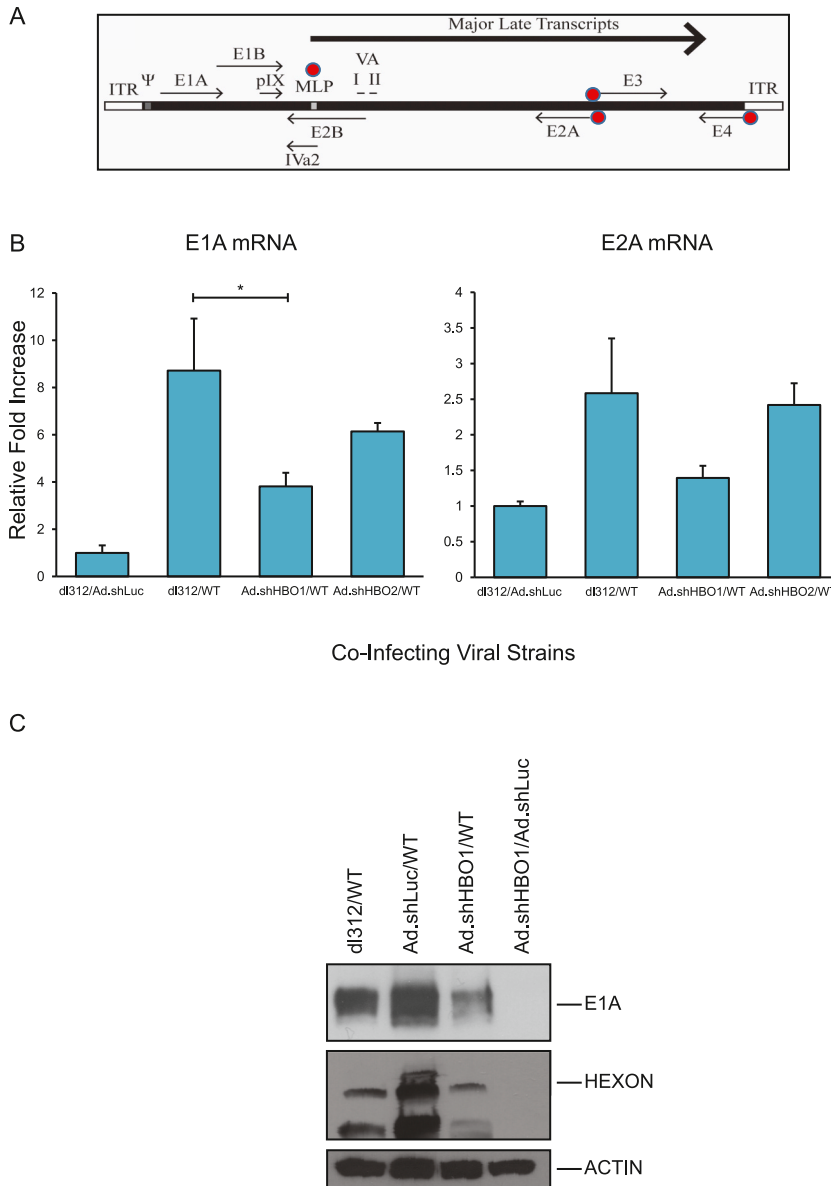


Fig. 2. Viral RNA and protein levels are reduced in HBO1 downregulated MCF10A cells. A. Schematic representation of the HAAdV genome with various transcriptional units indicated. Red dots mark viral promoters used in later ChIP experiments. B. Cells were first infected with controls or Ad. shRNA vectors targeting HBO1, then superinfected using the time points indicated (see Fig. 1A). Viral RNAs were prepared as described in Materials and Methods section. Viral mRNAs were quantified using RT-qPCR using the $\Delta\Delta C_t$ method versus cells infected only with *dl312/Ad.shLuc* control viruses as described in the Materials and Methods. Error bars represent standard deviation with * - $p \leq 0.05$; $n = 3$. C. Same as B except E1A and hexon protein levels were determined by Western blot. Uncropped blots are shown in supplemental figures. (For interpretation of the references to colour in this figure legend, the reader is referred to the Web version of this article.)

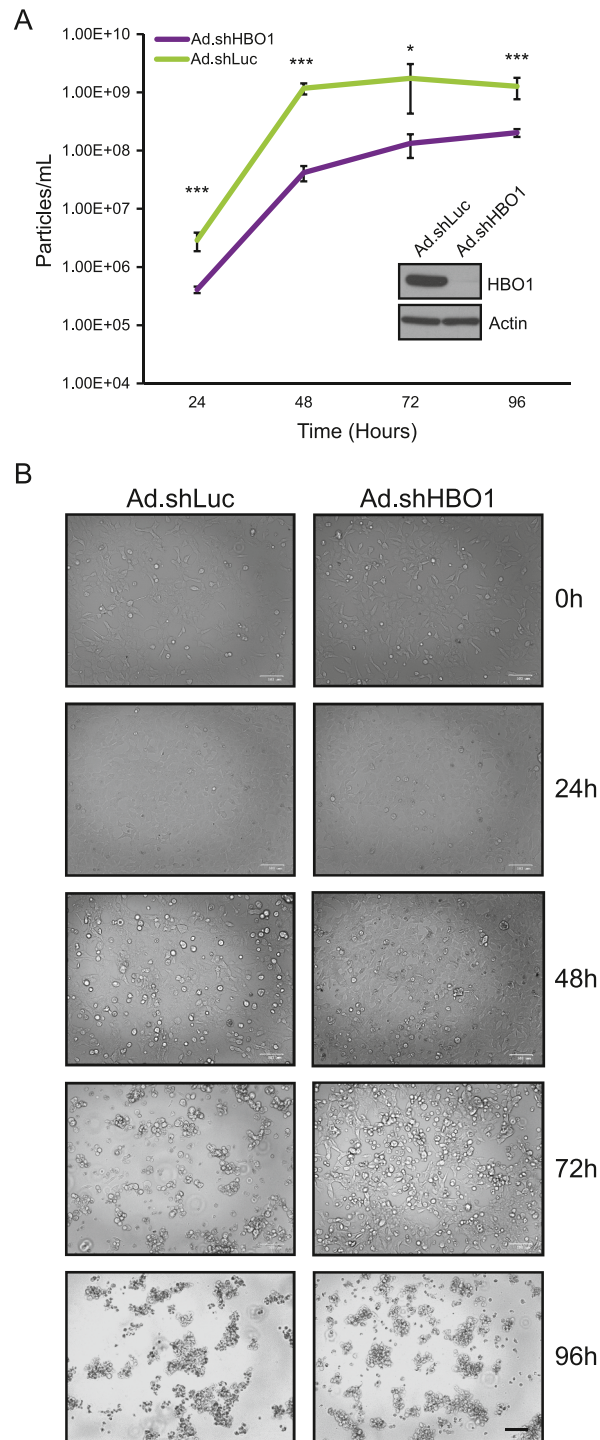
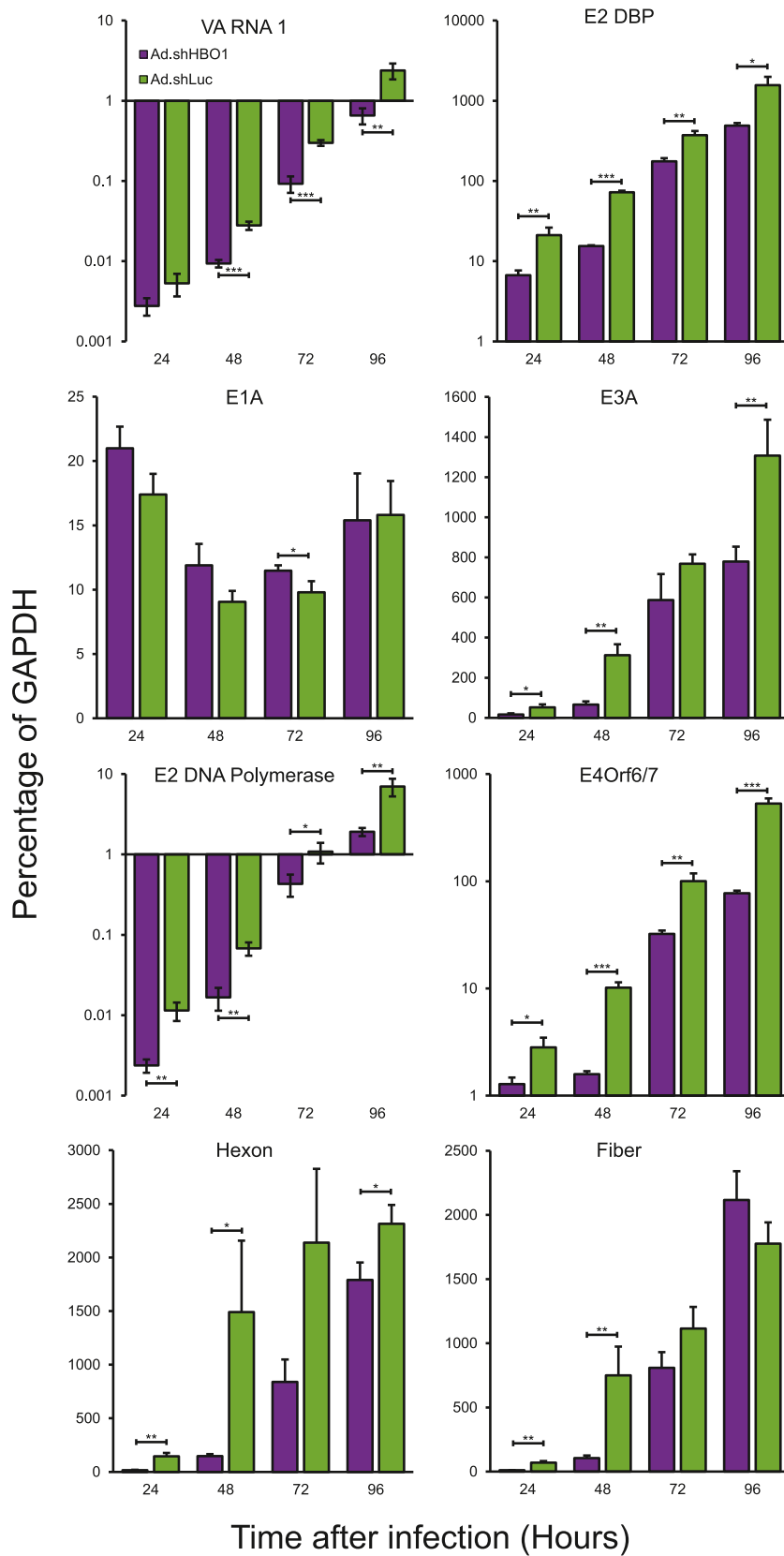


Fig. 3. Reduction of HBO1 affects HAdV growth and appearance of CPE in 293 cells. 293 cells were plated and infected at MOI 10 and then imaged and harvested in triplicate at the indicated time points. A. Viral particle quantification in 293 cells at the indicated time points in control (Ad.shLuc) or HBO1 (Ad.shHBO1) knockdown cells. Inset Western blot shows knockdown of HBO1 in 293 cells with ACTIN loading control, with uncropped Western blot images found in supplemental figures. Error bars represent standard deviation with * - $p \leq 0.05$, *** - $p \leq 0.001$; $n = 3$. B. Cytopathic effect in Ad.shHBO1 or Ad.shLuc infected 293 cells imaged in bright field using BioRad ZOE cell imager at 20 \times magnification. Bar represents 100 μ m.



(caption on next page)

Fig. 4. HBO1 knockdown reduces both early and late viral early gene expression. 293 cells were infected at an MOI of 10 with the indicated viral constructs for the lengths of time shown, before total RNA was extracted using the TRIzol method as described in the Materials and Methods. cDNA was produced using VIL0 Master Mix, and levels of the indicated RNAs were measured via RT-qPCR with human *GAPDH* mRNA as a reference. Levels of viral RNAs are shown as percentage of *GAPDH* mRNA. Each bar represents the average with * - $p \leq 0.05$, ** - $p \leq 0.01$; $n = 3$.

2. Results

2.1. Knockdown of HBO1 affects wild-type HAdV5 gene expression in MCF10A cells

Our efforts to create an HBO1 knock-out human cell line using CRISPR technology were unsuccessful (unpublished results). Therefore, to determine whether HBO1 is required for the efficient HAdV replication in non-tumorigenic human cells, we created two E1A deleted HAdV vectors expressing short hairpin RNAs (shRNAs) targeting two different coding regions of the human HBO1 mRNA (Ad.shHBO1 and Ad.shHBO2). We employed this approach instead of a more conventional siRNA use because we were unable to obtain satisfactory, or even significant, knockdown of HBO1 in a few different cell lines with commercially available, mRNA-validated siRNAs (data not shown). To determine the capacity of these HAdV vectors to downregulate endogenous HBO1 levels, MCF10A cells, an immortalized non-tumorigenic human breast epithelial cell line [25], were infected with the above mentioned HAdV shRNAs for 24 h then superinfected with WT virus or E1A negative HAdV variants as controls. Fig. 1A shows the infection strategy used in this experiment. We used this pre-infection/superinfection strategy in this experiment so that it matches with the protocol used in the phenotypic studies described below. However, comparable results were obtained without using WT virus in this experiment (data not shown). Twelve hours after second virus infection, cells were harvested and HBO1 mRNA levels were quantified using RT-qPCR. Data shown in Fig. 1B indicates that HBO1 mRNA levels decreased significantly in Ad.shHBO1 infected cells as compared to that of WT or control virus infections. Ad.shHBO2 virus was moderately effective in this regard, but this was not statistically significant. It is interesting to note that under these conditions, infection of WT virus did not affect endogenous HBO1 levels (compare bar 1 with bar 2, Fig. 1B). Next, we compared the HBO1 protein levels in Ad.shHBO1 virus infected cells with that of WT virus infected cells. Whole cell extracts prepared from cells infected with viruses as shown in Fig. 1A were analyzed by Western blots using an anti-HBO1 antibody. As shown in Fig. 1C Ad.shHBO1 vector downregulated endogenous HBO1 protein levels whereas Ad.shHBO2 was ineffective. We then examined whether HBO1 is required for HAdV gene expression using the infection strategy shown in Fig. 1A. Control viruses were also used for pre-infection and superinfections as detailed in the legend to Fig. 2. Cells were harvested and the total RNA was prepared. RNA levels were quantified to determine the expression of immediate-early E1A and early E2 DNA binding protein (DBP) genes by RT-qPCR. Fig. 2A shows the transcription map and the location of important viral genes and their promoters. Fig. 2B indicates that knockdown of HBO1 protein reduced RNA expression of both E1A and E2 DBP genes. We also determined whether reduced E1A mRNA reflects in the viral protein levels. As shown in Fig. 2C, in cells infected with Ad.shHBO1/WT combination, E1A and hexon protein levels were decreased considerably as compared to controls *dl312*/WT and Ad.shLuc/WT.

While the strategy of two virus infection of MCF10A cells overall worked well for the viral gene expression studies, it was difficult to use in the viral chromatin studies as we could not separate the association of HBO1 with the chromatin of the WT virus from that of the HAdVs expressing shRNAs. However, during the above studies, we also observed that Ad.shHBO1 virus replicated to significantly lower titers in 293 cells as compared to other viruses (such as the negative control Ad.shLuc), which provided the possibilities that we could use these cells to investigate HBO1 effects on viral chromatin.

2.2. Knockdown of HBO1 reduces virus growth

To investigate the effects of knockdown of HBO1 on HAdV growth we employed the viruses described above. Infection of 293 cells with Ad.shHBO1 resulted in robust reduction of HBO1 protein levels (Fig. 3A, see inset figure) as compared to that of control virus Ad.shLuc, that targets luciferase not normally found in mammalian cells. Reduction of HBO1 protein levels resulted in significant loss of viral titers observed throughout the viral replicative cycle (Fig. 3A). Viral titers were more than 10-fold lower at 24 h after infection and remained significantly lower throughout until the end at 96 h. Importantly, in HBO1-knockdown cells, the virus never reached the titers of control-treated cells despite complete cytopathic effect (CPE) observed (Fig. 3B). Furthermore, the time it took HBO1-knocked down cells to show CPE was delayed, with no significant CPE observed at 48 h after infection when CPE was observed in cells infected with Ad.shLuc at the same multiplicity of infection (MOI). These results suggest that functional HBO1 is required for efficient and maximal replication of HAdV.

2.3. Reduction of HBO1 affects viral gene expression

Since HBO1 is a chromatin remodeling factor and directly affects cellular gene expression, we wanted to determine whether the reduced viral titers observed when HBO1 was knocked down were due to reduced viral gene expression during infection. To investigate this, 293 cells were infected with Ad.shHBO1 or Ad.shLuc (control), total RNA was extracted, and viral mRNA levels were determined at 24, 48, 72, and 96 h after infection for all major viral transcriptional units (Fig. 4, see Fig. 2A for transcription map). Note that for these assays we wanted to determine the overall dynamics of viral gene transcription, therefore we present this data as a percentage of *GAPDH* mRNA as opposed to fold change versus control as was presented earlier. Except for E1A, which was provided by the cell line in *trans*, the levels of all viral early gene transcripts were significantly reduced in cells knocked down for HBO1 as compared to those

infected with the control virus (Fig. 4). This included the levels of the non-coding RNA VAI expressed by RNA polymerase III [26]. Similarly, late gene expression was also reduced in HBO1-knocked down cells, with hexon mRNA levels being particularly affected at 48 and 72 h with some recovery observed at 96 h after infection (Fig. 4). Overall, these results demonstrate that knockdown of HBO1 affects viral gene expression negatively, which may explain reduced virus growth.

2.4. Knockdown of HBO1 reduces histone H3 lysine 14 acetylation on viral promoters

Our results indicate that in HBO1-knocked down conditions the expression of viral genes is significantly compromised (Figs. 2 and 4). Therefore, we reasoned that this may be due impairment of viral chromatin remodeling when HBO1 is absent or reduced. HBO1 was

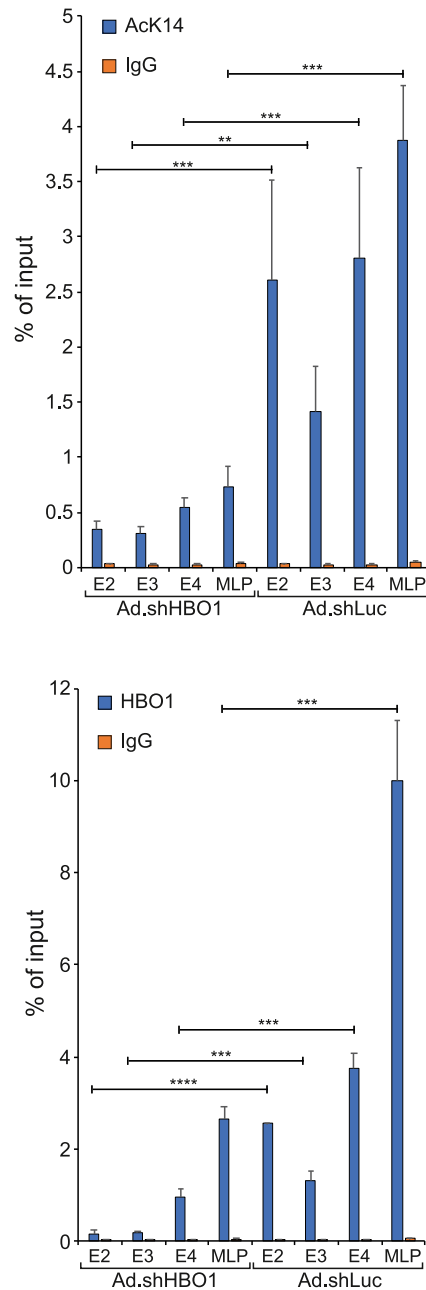


Fig. 5. HBO1 knockdown reduces histone H3 K14 acetylation within viral promoters. 293 cells were infected with the indicated viruses at an MOI of 10 for 24 h. Cells were then fixed, and ChIP was performed for acetylated histone H3 at K14 (top panel) or HBO1 (bottom panel) as described in the Materials and Methods. Anti-rat rabbit IgG antibody was used as a negative control immunoglobulin. Mean value of replicates is shown with error bars representing standard deviation with ** - $p \leq 0.01$, *** - $p \leq 0.001$, **** - $p \leq 0.0001$; $n = 3$.

previously shown to be a critical player in histone H3 K14 acetylation and gene expression [16]. We therefore wanted to determine whether reduction of HBO1 had any impact on acetylation of this residue on viral chromatin at promoters. To do this, 293 cells were infected with Ad.shHBO1 then chromatin was immunoprecipitated with an anti-acetyl K14 H3 or an IgG negative control antibody (Fig. 5; Fig. 2A shows the location of promoters on HAdV genome as red dots). Knockdown of HBO1 resulted in a significant reduction of H3K14 acetylation on all viral promoters tested, with the greatest effect observed for the E4 promoter and lowest effect observed on the E3 and the Major Late Promoter (MLP). Recruitment of HBO1 was also observed on all viral promoters analyzed (Fig. 5B) and it was significantly reduced with HBO1 knockdown, consistent with HBO1 reduction. The highest HBO1 occupancy was observed on the E2 promoter and lowest on E4. These results demonstrate that HBO1 is recruited to viral promoters and affects histone H3 acetylation of these regions, providing a potential mechanism for the reduced viral gene expression. These results also demonstrate that reduction of HBO1 protein leads to significant reduction of histone H3 K14 acetylation on viral promoters.

2.5. HBO1 localizes to viral replication centers during infection

The observation of differing effects on viral genes expressed in *cis* versus those expressed in *trans* in 293 cells suggests that the local environment affects the ability of HBO1 to selectively acetylate histones associated with viral chromatin. Similarly to what we have previously observed with splicing of E1A [27], HAdV replication occurs within nuclear compartments termed virus replication centers that foster viral gene expression and genome replication and these can be visualized with an antibody to the viral E2 DBP. We have therefore used immunofluorescence to visualize HBO1 within the nuclei of cells infected with *dl309*, a phenotypically WT variant of HAdV5 (Fig. 6). In infected and uninfected cells HBO1 was localized to the nucleoplasm, showing diffuse nuclear staining. Importantly, in infected cells that showed viral replication centers visualized with DBP staining, HBO1 was co-localizing to these centers, indicating some degree of increase in local concentration of HBO1 at sites of virus replication versus the general nucleoplasm. Together, these

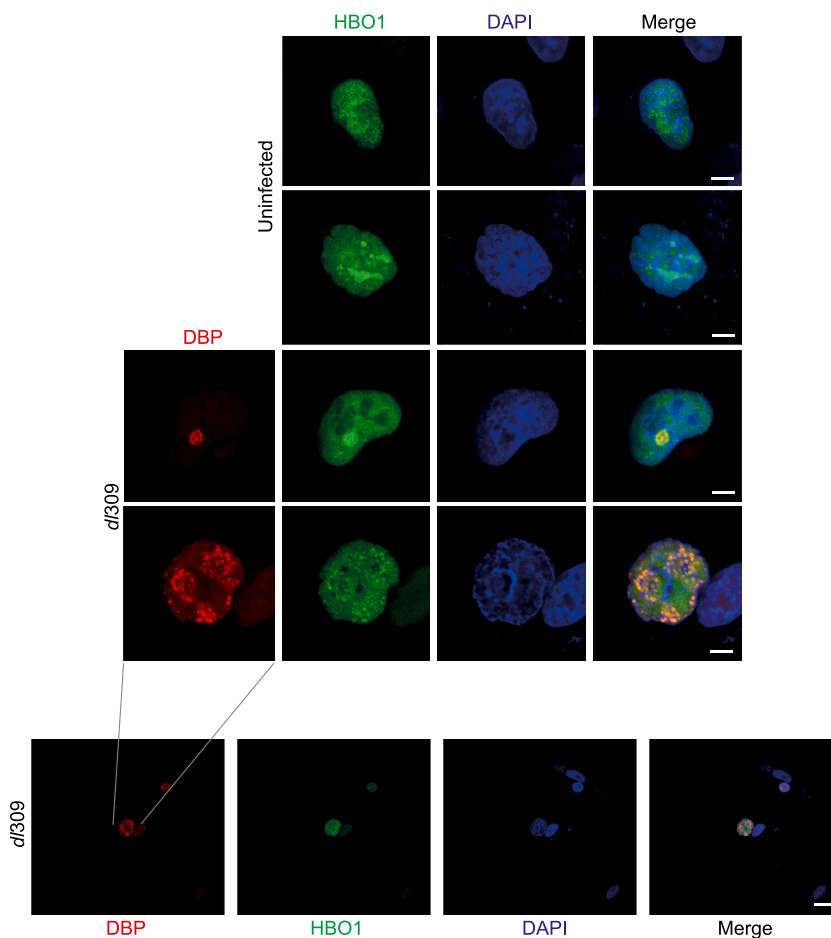


Fig. 6. HBO1 localizes to viral replication centers during infection. A549 cells were infected with *dl309* at an MOI of 10, fixed and stained for HBO1 (green) and DBP (red) 24 h after infection. DAPI was used as a nuclear counterstain. Uninfected cells were used as a negative control and were stained for HBO1 only. Images were acquired on a Zeiss LSM700 laser confocal microscope. Scale bar in the top 4 panels represents 5 μm while the scale bar in the bottom, zoomed out view, represents 20 μm . (For interpretation of the references to colour in this figure legend, the reader is referred to the Web version of this article.)

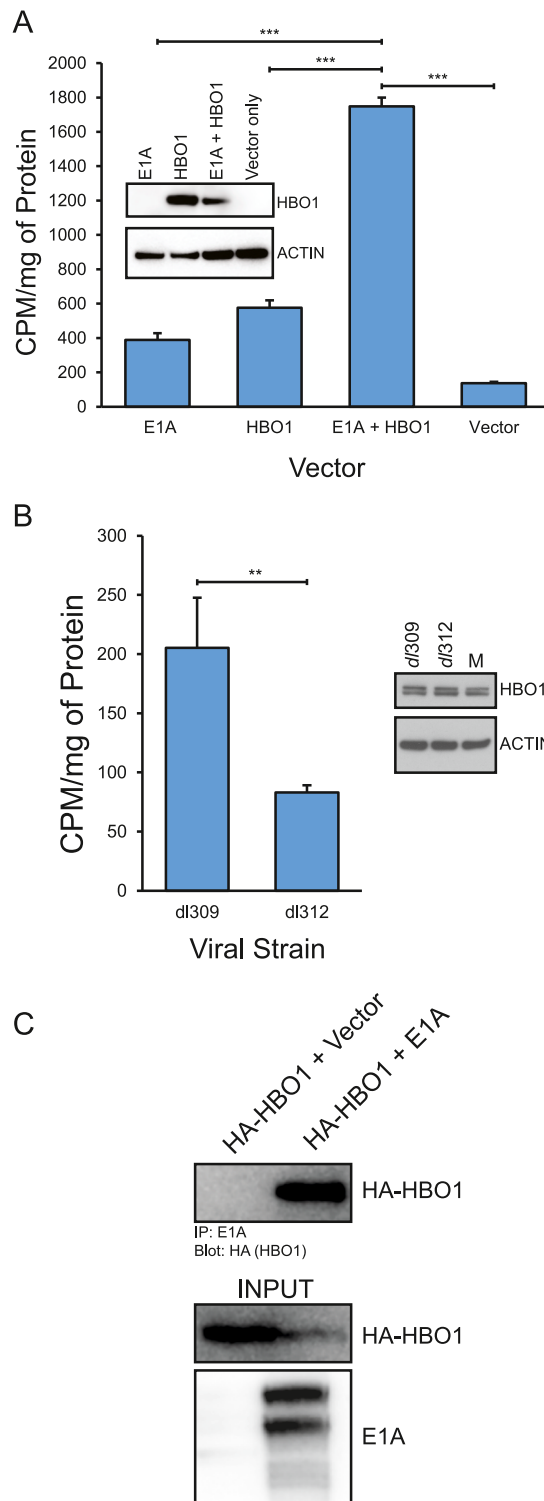


Fig. 7. E1A stimulates HBO1 HAT activity and binds to HBO1 in transient assays. **A.** E1A stimulates HBO1 HAT activity. 293 cells were transfected with 10 μ g of FLAG epitope tagged CMV promoter/enhancer driven HBO1 expression vector along with equal quantities of an E1A expression plasmid for 24 h. Empty vector DNA was included where appropriate to equalize the amount of DNA during transfection. Acetyltransferase activity was measured 24 h after transfection as described in the Materials and Methods. Inset shows the levels of transfected FLAG-tagged HBO1 or ACTIN, which was used as a loading control. Error bars represent standard deviation with *** - $p \leq 0.001$; $n = 3$. Uncropped blots are shown in supplemental figures. **B.** Left panel: MCF10A cells were infected with the indicated viruses for 20 h, cells were then lysed, HBO1 was immunoprecipitated, and acetyltransferase activity was measured. Right panel: Cells infected for acetyltransferase activity were also subject to protein expression analysis

for endogenous HBO1 and ACTIN loading control, M – mock infected. Error bars represent standard deviation with ** - $p \leq 0.01$; $n = 3$. Uncropped blots are shown in supplemental figures. C. E1A interacts with HBO1. HT1080 cells were co-transfected with E1A and HA-tagged HBO1, or E1A and the HA-tagged empty vector (pCAN-HA) for 24 h. Cells were lysed and immunoprecipitated for E1A using M73 hybridoma supernatant. Immunoprecipitations were resolved on NuPAGE BOLT 4–12% gradient gels and visualized using ECL using the Azure C600 digital imager. 1.5% of input is also shown. Uncropped blots are shown in supplemental figures.

results demonstrate that HBO1 localizes to viral replication centers, which may facilitate more efficient acetylation of viral genomes.

2.6. E1A stimulates HBO1 acetyltransferase activity

E1A has previously been shown to associate with all HAdV promoters and stimulate transcription [28]. It is well documented that p300 is recruited to the HAdV promoters along with E1A, but E1A dissociates from the promoter shortly after E1A-mediated transcriptional activation [22]. Furthermore, E1A binds directly to the pocket domain of p300, to which many cellular and viral proteins also bind [29]. However, it is not entirely clear whether E1A stimulates p300 HAT activity. We investigated whether E1A stimulates HBO1 acetyltransferase activity as one possible mechanism by which HBO1 participates in histone acetylation at viral promoters by overexpression of E1A. In 293 cells, E1A overexpression by transient transfection for 24 h together with FLAG-tagged HBO1 led to a significant enhancement of HBO1 acetyltransferase activity (Fig. 7A) despite E1A overexpression leading to reduced levels of transfected HBO1 as compared to when E1A was not overexpressed (Fig. 7A). Likewise, infection of MCF10A cells with *dl309* for 20 h followed by detection of native HBO1 acetyltransferase activity led to a significant increase in endogenous activity (Fig. 7B), without affecting endogenous HBO1 protein levels (Fig. 7B, right panel). These results suggest that E1A may affect HBO1 acetyltransferase activity via an unknown mechanism.

Earlier studies have shown that E1A binds to several HAT proteins while activating cellular and viral promoters. Therefore, we asked whether E1A binds to HBO1. To address this, HT1080 cells were co-transfected with plasmids expressing HA-tagged HBO1 and an empty control plasmid, or E1A and HA-tagged HBO1 together, cell lysates were subsequently immunoprecipitated for E1A using M73 monoclonal antibody (Fig. 7C). E1A efficiently immunoprecipitated HBO1, indicating that these two proteins interact. It is unclear why levels of HBO1 were reduced in the presence of E1A; however, this was a consistent observation (as observed in Fig. 7A) with repeat experiments and does not alter the conclusions.

3. Discussion

In the present study we report on the influence of HBO1 acetyltransferase on the replication of HAdV5. Knockdown of HBO1 had a significant negative effect on the overall ability of the virus to replicate. This was based on delayed appearance of CPE (48 h in control cells and 72 h in HBO1-knockdown cells in Fig. 3) and overall reduced viral titers (~10-fold reduction) by the end point of the assay (96 h) when all cells were killed. HBO1 was found localized with viral replication centers and was associated with viral chromatin. Reduction of HBO1 protein levels resulted in reduced viral gene expression, likely caused by reduced acetylation of histone H3 K14. Lastly, we observed that during infection, HBO1 acetyltransferase activity was stimulated and this may have been driven, in part, by an interaction with E1A.

The negative impact of HBO1 knockdown on adenovirus replication is not unsurprising considering the many critical cellular processes that HBO1 participates in, including many that are of importance to the virus. These processes include DNA replication [14, 15], gene transcription [30], DNA damage response [31], and immune response [32]. Many of these processes are directly or indirectly deregulated during HAdV infection by the virus. Virus growth was significantly lower in HBO1 downregulated cells, likely this was a consequence of significant reduction in viral gene expression in knocked down cells. In cells knocked down for HBO1 there was a substantial loss of histone H3 acetylation on K14, a mark associated with activated gene expression [33]. Unsurprisingly, this resulted in a marked and significant reduction in viral gene transcription. Interestingly, HBO1 occupancy was highest on the E2 viral promoter, although this did not directly translate into higher levels of acetylation detected at this promoter. This observation may, nevertheless, hint at transcriptional coupling of the cell cycle regulatory mechanisms that rely on transcription factor recruitment to cell cycle regulated genes and recruitment of HBO1 to viral promoters, regulated by the same factors. Indeed, recruitment of HBO1 was lowest at the E4 promoter, which we previously observed to be activated at the same time as E1A and therefore likely not directly driven by E1A [17] early in infection. This suggests that regulation of HBO1 recruitment to promoters, or other sites on chromatin may be regulated by the same stimuli that drive DNA replication.

Interestingly, we observed that the activation of the *E1A* gene expression was not affected by knockdown of HBO1 in 293 cells but had a negative effect on expression of E1A from the viral genome in normal MCF10A cells. In our analysis of gene expression in 293 cells, E1A was provided *in trans* by the cell line from the integrated left end of the adenoviral genome, while in MCF10A cells infected with *dl309*, E1A was expressed directly from the viral genome, but not in *dl312* infected cells as this virus is deleted for E1A. These observations suggest that the sequence of the promoter along with the nucleoplasm microenvironment, local to where the sequence is located, likely influence recruitment of HBO1 to the promoter region and histone acetylation. Since HBO1 is co-localized with viral replication centers, it is plausible that its local concentration and availability is higher than other regions within the nucleus, enhancing its recruitment to promoters and effects on gene expression. The *E1A* gene present in 293 cells does not, generally, co-localize with viral replication centers early in infection [27] and therefore would not benefit from the changes to the local microenvironment that these centers provide, resulting in suboptimal gene expression. This parallels what we have previously observed with

E1A RNA splicing, where E1A RNA expressed from the genome of 293 cells was spliced differentially to that expressed from the viral genome [27].

In this report, we showed that increased levels of E1A stimulates HBO1 HAT activity without increasing its levels which is surprising and intriguing. We are not aware of any clear example of E1A stimulation of a HAT protein. We also showed that E1A can bind to HBO1 consistent with the general mechanism by how viral transactivators stimulate transcription using HAT proteins. At present, we do not know the mechanism(s) by which E1A stimulates the HBO1 catalytic activity. One possibility is that more E1A would stimulate the cell cycle to some degree (as we have previously observed in HeLa cells; unpublished results) and this would indirectly stimulate HBO1 acetyltransferase activity. Another possibility is that E1A can directly drive HBO1 acetyltransferase activity and with more E1A more activity is observed. The latter possibility is intriguing, as E1A itself is phosphorylated by CDK1 [34] and HBO1 is also phosphorylated by the same kinase [35]. Mutation of the CDK1 phosphorylation site on HBO1 leads to cell cycle arrest at the G₁/S phase, impairment of replication fork firing, and DNA replication. It is not clear whether this phosphorylation affects HBO1 catalytic activity but one possibility is that via a transient interaction E1A is able to drive this HBO1 phosphorylation and stimulate its catalytic activity. Alternatively, E1A may simply be upregulating factors present in the HBO1 complex and/or other cellular factors that directly affect HBO1 catalytic activity as it drives cells into S-phase. For example, HBO1 exists as a complex with several other proteins including ING4/5, hEAF6, and the scaffold protein JADE1/2/3 which is important for HBO1 function. HBO1 when complexed with JADE scaffold protein targets H4 histone tails to acetylate lysines at residues 5, 8, 12 (H4K5/8/12ac) but can switch its scaffold protein to BRPF then target H3 tails to acetylate lysines residues 14 and 23 (H3K14/23ac). So, it is conceivable that E1A may increase the levels of these factors including the scaffold proteins JADE or BRPF that promote HBO1 protein activity. Ultimately, much further work needs to be carried out to fully understand how this occurs. Furthermore, it would be of future interest to determine whether acetylation of histone H4 on viral chromatin is impacted by HBO1 and E1A, and whether it affects viral genome replication.

It is known that HAT proteins such as p300 and HBO1 acetylate proteins other than chromatin histones. With the exception of acetylation of E1A [29], and adenovirus proteins VII and V [36,37], acetylation of other HAdV encoded proteins has not been reported. So, it is possible that the HBO1 complex may also acetylate additional virus-encoded proteins that can impact on viral replication. One of the viral proteins, protein VII, plays an important role in viral replication by binding tightly to viral DNA and inhibiting viral DNA transcription after its nuclear entry [38,39]. To enable viral early gene transcription, protein VII undergoes posttranslational modifications including acetylation immediately after infection, which allows its release from DNA and enables transcription [37,40]. This raises the intriguing possibility that protein VII may be a substrate for the HBO1 HAT complex. It will be interesting to explore this possibility in future studies.

In conclusion the present study has identified an important role for the HBO1 acetyltransferase in HAdV replication. Knockdown of HBO1 had a negative impact on viral replication, chromatin modification, and gene expression. E1A was also observed to stimulate the enzymatic activity of HBO1 via an unknown mechanism. Considering the important role of HBO1 in regulation of cellular growth, our studies provide further insights into oncogenic properties of small DNA tumor virus proteins and shed further light on how these master reprogrammers alter cellular homeostasis.

4. Materials and methods

4.1. Acetyltransferase activity assay

To determine whether E1A stimulates HBO1 HAT activity, 293 cells were co-transfected with plasmids expressing FLAG-HBO1 from CMV promoter/enhancer and WT E1A. After 48 h (or the time indicated in figure legends), total cell extracts were immunoprecipitated using anti-FLAG or anti-HBO1 antibody and equal amounts of protein were assayed *in vitro* for HAT activity using ³H acetyl CoA as the donor of acetyl group and a synthetic peptide corresponding to the N-terminal 20 aa of H3 as substrate [41]. The radioactivity present in the peptide was quantified using a liquid scintillation counter [41].

4.2. Antibodies

Mouse monoclonal M73 anti-E1A antibody was used for E1A Western blots and was previously described [42]. Mouse monoclonal anti-72k E2 DNA Binding Protein (DBP) antibody was previously described [43] and was used at a dilution of 1:400 for immunofluorescence. Anti-Adenovirus hexon protein antibody was purchased from Abcam (ab252760). Anti-HBO1 and anti-histone H3K14Ac were purchased from Abcam (cats. ab124993 and ab52948, respectively) and were used according to manufacturer's specifications. Secondary antibodies were purchased from Jackson ImmunoResearch, including Alexa 488 and Alexa 594 conjugated secondary antibodies used in fluorescent imaging.

4.3. Cells and viruses

The 293 (ATCC# CRL-1573), HT1080 (ATCC# CCL-121), and A549 (ATCC# CCL-185) cells were grown in Dulbecco's Modified Eagle's Medium (HyClone) supplemented with 10% fetal bovine serum (Seradigm), and streptomycin and penicillin (HyClone). Growth media for MCF10A cells (ATCC# CRL-10317) were as described before [25]. All virus infections were carried out in serum-free media for 1 h at an MOI of 10 unless specified otherwise, after which saved complete media was added without removal of the infection media. HAdV5 *dl309*, and *dl312* were previously described [44,45].

Ad.shScr which contains a scrambled shRNA under the control of U6 promoter was purchased from Vector Biolabs (Cat. No. 1122).

Ad.shHBO1 and Ad.shHBO2 viruses were constructed in our laboratory using Invitrogen BLOCK-iT Adenoviral RNAi Expression System (Cat. No: K494100). Ad.shHBO1 contains following oligonucleotide sequences.

Forward:

GATCCGGGATAAGCAGCATAGAAGAAATCAAGAGTTTCTTCTATCGCTTATCCCTTTTG.

Reverse:

AATTCAAAAAGGGATAAGCAGATAGAAGAAACTCTTGATTTCTTCTATCTGCTTATCCCG with *Bam*HI at the 5' end and *Eco*RI at the 3' end as the cloning sites (shown underlined). Ad.shHBO2 contains:

Forward:

GATCCGCTCAAATACTGGAAGGGAATCAAGAGTTCCTTCCAGTATTTGAGCTTTTGTG.

Reverse:

AATTCAAAAGCTCAATACTGGAAGGGAATCAAGAGTTCCTTCCAGTATTTGAGC.

The oligos were annealed by heating to 100 °C and slowly cooled, then subcloned into the recombination vector and then co-transformed with the viral backbone plasmid for recombination according to manufacturer instructions (Invitrogen). The 293 cells were then transfected with recovered full-length linearized viral plasmid and when the cells showed cytopathic effect, the cells were harvested and lysed by freeze-thawing three times to liberate the viruses. The cell lysate was subsequently used to infect new 293 cells for expansion, and this virus was collected and used as stock for further experiments. Details of Ad.shLuc virus were previously published [23]. For the experiments shown in Figs. 1 and 2, the virus stocks were titered using Clontech Labs 3P Adeno-X Rapid Titer.

4.4. Chromatin immunoprecipitation

Chromatin immunoprecipitation (ChIP) was carried out essentially as previously described [3,20]. 293 cells were infected with the indicated adenoviruses at MOI of 10 and harvested 24 h after infection for ChIP analysis. Rabbit anti-rat antibody was used as a negative control IgG.

PCR reactions were carried out for HAdV5 early and major late promoters using EvaGreen Master Mix for ddPCR (BioRad) with 3% of total ChIP DNA as template according to manufacturer's instructions using a BioRad QX200 digital droplet PCR instrument (BioRad). The annealing temperature used was between 55 °C and 65 °C, depending on the primer set, and 40 cycles were run. Primers for viral promoters were previously described [46].

4.5. Cytopathic effect

As previously described by Costa et al. [47] and Graves et al. [27], 293 cells were plated and then subsequently infected at a MOI 10 with either Ad.shHBO1 or Ad.shLuc in serum free media for 1 h. At the indicated time points, cells were imaged in the bright field at 20× magnification using the BioRad ZOE cell imager.

4.6. E1A binding assay

Immunoprecipitations (IP) were carried out as previously described [48]. Briefly, transfected HT1080 cells were lysed in NP-40 lysis buffer (0.5% NP-40, 50 mM Tris [pH 7.8], 150 mM NaCl) supplemented with a protease inhibitor cocktail (MilliporeSigma). Cell lysate containing 1 mg of total protein was used for IP with the monoclonal M73 anti-E1A antibody for 1 h at 4 °C. Beads were washed 3 times in lysis buffer and resuspended in sample buffer, boiled for 10 min and resolved on 4–12% gradient NuPAGE BOLT gel. Gels were transferred to PVDF and blotted for the indicated proteins.

4.7. Gene expression analysis

The 293 cells were infected in triplicate with indicated viral constructs at MOI 10 and harvested at indicated timepoints. Total RNA was extracted using TRIzol Reagent (MilliporeSigma) according to manufacturer instructions. Any remaining genomic DNA was removed using Invitrogen TURBO DNA-free Kit. RNA yields were quantified via spectrophotometry (Molecular Devices SpectraMax iD3) and 1 µg from each sample was used to generate complementary DNA with SuperScript IV VILO Master Mix (Invitrogen), according to manufacturer guidelines. This cDNA was subsequently used for real-time expression analysis with the BioRad CFX96 real-time thermal cycler and Applied Biosystems SYBR Select Master Mix for CFX, with an annealing step of 60 °C for 1 min. Expression data were normalized to *glyceraldehyde-3-phosphate dehydrogenase (GAPDH)* mRNA levels when the data is presented as percentage of *GAPDH*, or to 18S rRNA when the data is presented as fold change. For fold change results, the $\Delta\Delta$ Ct method was used.

4.8. Immunofluorescence

A549 cells were plated at low density (~40,000 cells per chamber) on chamber slides (Nalgene Nunc), and subsequently infected as described. Twenty-four hours after infection, cells were fixed in 4% formaldehyde, permeabilized in 0.1% Triton, blocked in blocking buffer (1% normal goat serum, 1% BSA, 0.2% Tween-20 in PBS) and stained with specific primary antibodies and fluorescent secondary antibodies. After staining and extensive washing, slides were mounted using Prolong Gold with DAPI (Invitrogen) and imaged using Zeiss LSM700 confocal laser scanning microscope. Images were analyzed using Zeiss ZEN software package.

4.9. Primers

Primers used were purchased from Integrated DNA Technologies, and their sequences are as previously indicated [46], with six exceptions, listed here:

E2B F – TGCCGACAAAAACCAAACCC
 E2B R – TGTC AAGCTTGGTGGCAAAC
 E4-Orf3 F – CTCGAGTTATTCCAAAAGATTATCCAAAAC
 E4-Orf3 R – GAATTCATTCGCTGCTTGAGGCTGAA
 Fiber F – ATGCTTGCGCTCAAATGGG
 Fiber R – TTTTGTAGAGGTGGGCTCAC

4.10. Statistical analysis

Statistical analysis for all experiments was performed with GraphPad Prism v5 software using a two-tailed Student's *t*-test. *P*-values of ≤ 0.05 were considered statistically significant. The mean is shown for all experimental results with error bars representing standard deviation of all biological and technical replicates. Quantity of biological replicates is indicated with an "n" in the figure legends.

4.11. Virus growth assay

The 293 cells were plated and 24 h later infected in triplicate at a MOI 10 with either Ad.shHBO1 or Ad.shLuc in serum free media for 1 h. At the indicated time points the infected cells were harvested and then freeze-thawed three times. Non-encapsulated DNA, including free viral genomic DNA, was degraded by treating the lysates with DNase I for 1 h at 37 °C, followed by DNase I inactivation using the TurboDNase kit from Invitrogen. Subsequently, all proteins were degraded using 1 h proteinase K treatment at 42 °C to liberate encapsulated viral genomic DNA. Viral genomic DNA was then purified using BioBasic DNA purification kit. Viral genomes were then quantified by quantitative real-time PCR with a serial dilution of pXC1 plasmid (having the E1 region cloned in it) serving as the standard curve as previously described [49] using the BioRad CFX96 real-time thermocycler (BioRad).

Data availability

No large data sets were generated in this study as such none were submitted to a repository. Data included and/or referenced in the article.

CRedit authorship contribution statement

Heba Kamel: Visualization, Methodology, Formal analysis. **Varsha Shete:** Methodology, Formal analysis. **Sayikrushna Gadamsetty:** Methodology, Formal analysis. **Drayson Graves:** Visualization, Methodology, Formal analysis. **Scott Bachus:** Visualization, Methodology, Formal analysis. **Nikolas Akkerman:** Visualization, Methodology, Formal analysis. **Peter Pelka:** Writing – review & editing, Writing – original draft, Visualization, Supervision, Project administration, Methodology, Funding acquisition, Formal analysis, Data curation, Conceptualization. **Bayar Thimmapaya:** Writing – review & editing, Writing – original draft, Validation, Project administration, Funding acquisition, Formal analysis, Data curation, Conceptualization.

Declaration of competing interest

The authors declare the following financial interests/personal relationships which may be considered as potential competing interests: Bayar Thimmapaya reports financial support was provided by National Institutes of Health. Peter Pelka reports financial support was provided by Canadian Institutes of Health Research. Peter Pelka reports financial support was provided by Natural Sciences and Engineering Research Council of Canada. If there are other authors, they declare that they have no known competing financial interests or personal relationships that could have appeared to influence the work reported in this paper.

Acknowledgments

This work was supported by NIH grant R21AI094296 to BT. This work was supported by a grant from the Natural Sciences and Engineering Research Council (Grant number: RGPIN/05366-2019), and grants from the Canadian Institutes of Health Research to PP. (Grant numbers: PJT-173376 and PJT-166198). PP thanks Stanisława Pelka for invaluable support and assistance and Ryszard Pelka for inspiration and curiosity, and for their critical feedback on the manuscript. Ancy Jacob, Manasa Sagaram, Yuhi Zao, Eva Bednarki, and Disha Malhotra for help in certain experiments.

Appendix A. Supplementary data

Supplementary data to this article can be found online at <https://doi.org/10.1016/j.heliyon.2024.e28827>.

References

- [1] A.J. Berk, *Fields Virology*, sixth ed., Wolters Kluwer/Lippincott Williams & Wilkins Health, 2013.
- [2] P. Pelka, J.N. Ablack, G.J. Fonseca, A.F. Yousef, J.S. Mymryk, Intrinsic structural disorder in adenovirus E1A: a viral molecular hub linking multiple diverse processes, *J. Virol.* 82 (2008) 7252–7263, <https://doi.org/10.1128/JVI.00104-08>. JVI.00104-08 [pii].
- [3] P. Pelka, J.N. Ablack, J. Torchia, A.S. Turnell, R.J. Grand, J.S. Mymryk, Transcriptional control by adenovirus E1A conserved region 3 via p300/CBP, *Nucleic Acids Res.* 37 (2009) 1095–1106, <https://doi.org/10.1093/nar/gkn1057>, gkn1057 [pii].
- [4] J.N. Ablack, M. Cohen, G. Thillainadesan, G.J. Fonseca, P. Pelka, J. Torchia, J.S. Mymryk, Cellular GCN5 is a novel regulator of human adenovirus E1A-conserved region 3 transactivation, *J. Virol.* 86 (2012) 8198–8209, <https://doi.org/10.1128/JVI.00289-12>.
- [5] P. Pelka, J.N. Ablack, M. Shuen, A.F. Yousef, M. Rasti, R.J. Grand, A.S. Turnell, J.S. Mymryk, Identification of a second independent binding site for the pCAF acetyltransferase in adenovirus E1A, *Virology* 391 (2009) 90–98, <https://doi.org/10.1016/j.virol.2009.05.024>. S0042-6822(09)00332-8 [pii].
- [6] D.C. Bedford, P.K. Brindle, Is histone acetylation the most important physiological function for CBP and p300? *Aging (Albany NY)* 4 (2012) 247–255, <https://doi.org/10.18632/aging.100453>.
- [7] E. Koutelou, A.T. Farria, S.Y.R. Dent, Complex functions of Gcn5 and Pcaf in development and disease, *Biochim Biophys Acta Gene Regul Mech* 1864 (2021) 194609, <https://doi.org/10.1016/j.bbagr.2020.194609>.
- [8] J.L. Dahlin, X. Chen, M.A. Walters, Z. Zhang, Histone-modifying enzymes, histone modifications and histone chaperones in nucleosome assembly: lessons learned from Rtt109 histone acetyltransferases, *Crit. Rev. Biochem. Mol. Biol.* 50 (2015) 31–53, <https://doi.org/10.3109/10409238.2014.978975>.
- [9] M.R. Parthun, Histone acetyltransferase 1: more than just an enzyme? *Biochim. Biophys. Acta* 1819 (2012) 256–263, <https://doi.org/10.1016/j.bbagr.2011.07.006>.
- [10] L. Pillus, MYSTs mark chromatin for chromosomal functions, *Curr. Opin. Cell Biol.* 20 (2008) 326–333, <https://doi.org/10.1016/j.ceb.2008.04.009>.
- [11] R. Lan, Q. Wang, Deciphering structure, function and mechanism of lysine acetyltransferase HBO1 in protein acetylation, transcription regulation, DNA replication and its oncogenic properties in cancer, *Cell. Mol. Life Sci.* 77 (2020) 637–649, <https://doi.org/10.1007/s00018-019-03296-x>.
- [12] M.E. Lalonde, N. Avvakumov, K.C. Glass, F.H. Joncas, N. Saksouk, M. Holliday, E. Paquet, K. Yan, Q. Tong, B.J. Klein, et al., Exchange of associated factors directs a switch in HBO1 acetyltransferase histone tail specificity, *Genes Dev.* 27 (2013) 2009–2024, <https://doi.org/10.1101/gad.223396.113>.
- [13] V. Sapountzi, J. Cote, MYST-family histone acetyltransferases: beyond chromatin, *Cell. Mol. Life Sci.* 68 (2011) 1147–1156, <https://doi.org/10.1007/s00018-010-0599-9>.
- [14] B. Miotto, K. Struhl, HBO1 histone acetylase activity is essential for DNA replication licensing and inhibited by Geminin, *Mol. Cell.* 37 (2010) 57–66, <https://doi.org/10.1016/j.molcel.2009.12.012>.
- [15] M. Iizuka, B. Stillman, Histone acetyltransferase HBO1 interacts with the ORC1 subunit of the human initiator protein, *J. Biol. Chem.* 274 (1999) 23027–23034, <https://doi.org/10.1074/jbc.274.33.23027>.
- [16] A.J. Kueh, M.P. Dixon, A.K. Voss, T. Thomas, HBO1 is required for H3K14 acetylation and normal transcriptional activity during embryonic development, *Mol. Cell Biol.* 31 (2011) 845–860, <https://doi.org/10.1128/MCB.00159-10>.
- [17] L. Crisostomo, A.M. Soriano, M. Mendez, D. Graves, P. Pelka, Temporal dynamics of adenovirus 5 gene expression in normal human cells, *PLoS One* 14 (2019) e0211192, <https://doi.org/10.1371/journal.pone.0211192>.
- [18] A.J. Berk, Recent lessons in gene expression, cell cycle control, and cell biology from adenovirus, *Oncogene* 24 (2005) 7673–7685, <https://doi.org/10.1038/sj.onc.1209040>, 1209040 [pii].
- [19] C.R. King, A. Zhang, T.M. Tessier, S.F. Gameiro, J.S. Mymryk, Hacking the cell: network intrusion and exploitation by adenovirus E1A, *mBio* 9 (2018), <https://doi.org/10.1128/mBio.00390-18>.
- [20] S. Bachus, N. Akkerman, L. Fulham, D. Graves, R. Helwer, J. Rempel, P. Pelka, ARGLU1 enhances promoter-proximal pausing of RNA polymerase II and stimulates DNA damage repair, *Nucleic Acids Res.* (2024), <https://doi.org/10.1093/nar/gkae208>.
- [21] P. Pelka, M.S. Miller, M. Cecchini, A.F. Yousef, D.M. Bowdish, F. Dick, P. Whyte, J.S. Mymryk, Adenovirus E1A directly targets the E2F/DP-1 complex, *J. Virol.* 85 (2011) 8841–8851, <https://doi.org/10.1128/JVI.00539-11>. JVI.00539-11 [pii].
- [22] R.K. Kadeppagari, N. Sankar, B. Thimmappaya, Adenovirus transforming protein E1A induces c-Myc in quiescent cells by a novel mechanism, *J. Virol.* 83 (2009) 4810–4822, <https://doi.org/10.1128/JVI.02145-08>.
- [23] N. Sankar, S. Baluchamy, R.K. Kadeppagari, G. Singhal, S. Weitzman, B. Thimmappaya, p300 provides a corepressor function by cooperating with YY1 and HDAC3 to repress c-Myc, *Oncogene* 27 (2008) 5717–5728, <https://doi.org/10.1038/ncr.2008.181>.
- [24] G. Singhal, E. Leo, S.K. Setty, Y. Pommier, B. Thimmappaya, Adenovirus E1A oncogene induces rereplication of cellular DNA and alters DNA replication dynamics, *J. Virol.* 87 (2013) 8767–8778, <https://doi.org/10.1128/JVI.00879-13>.
- [25] H.D. Soule, T.M. Maloney, S.R. Wolman, W.D. Peterson Jr., R. Brenz, C.M. McGrath, J. Russo, R.J. Pauley, R.F. Jones, S.C. Brooks, Isolation and characterization of a spontaneously immortalized human breast epithelial cell line, MCF-10, *Cancer Res.* 50 (1990) 6075–6086.
- [26] B. Thimmappaya, N. Jones, T. Shenk, A mutation which alters initiation of transcription by RNA polymerase III on the Ad5 chromosome, *Cell* 18 (1979) 947–954, [https://doi.org/10.1016/0092-8674\(79\)90207-1](https://doi.org/10.1016/0092-8674(79)90207-1).
- [27] D. Graves, N. Akkerman, S. Bachus, P. Pelka, Differential splicing of human adenovirus 5 E1A RNA expressed in cis versus in trans, *J. Virol.* 95 (2021), <https://doi.org/10.1128/JVI.02081-20>.
- [28] J.R. Frost, M. Mendez, A.M. Soriano, L. Crisostomo, O. Olanubi, S. Radko, P. Pelka, Adenovirus 5 E1A-mediated suppression of p53 via FUBP1, *J. Virol.* 92 (2018), <https://doi.org/10.1128/JVI.00439-18>.
- [29] R.H. Goodman, S. Smolik, CBP/p300 in cell growth, transformation, and development, *Genes Dev.* 14 (2000) 1553–1577.
- [30] L. MacPherson, J.N. Anokye, M.M. Yeung, E.Y.N. Lam, Y.C. Chan, C.F. Weng, P. Yeh, K. Knezevic, M.S. Butler, A. Hoegl, et al., HBO1 is required for the maintenance of leukaemia stem cells, *Nature* 577 (2020) 266–270, <https://doi.org/10.1038/s41586-019-1835-6>.
- [31] H. Niida, R. Matsunuma, R. Horiguchi, C. Uchida, Y. Nakazawa, A. Motegi, K. Nishimoto, S. Sakai, T. Ohhata, K. Kitagawa, et al., Phosphorylated HBO1 at UV irradiated sites is essential for nucleotide excision repair, *Nat. Commun.* 8 (2017) 16102, <https://doi.org/10.1038/ncomms16102>.
- [32] R. Contzler, A. Regamey, B. Favre, T. Roger, D. Hohl, M. Huber, Histone acetyltransferase HBO1 inhibits NF-kappaB activity by coactivator sequestration, *Biochem. Biophys. Res. Commun.* 350 (2006) 208–213, <https://doi.org/10.1016/j.bbrc.2006.09.030>.
- [33] K. Karmodiya, A.R. Krebs, M. Oulad-Abdelghani, H. Kimura, L. Torra, H3K9 and H3K14 acetylation co-occur at many gene regulatory elements, while H3K14ac marks a subset of inactive inducible promoters in mouse embryonic stem cells, *BMC Genom.* 13 (2012) 424, <https://doi.org/10.1186/1471-2164-13-424>.
- [34] A. Mal, A. Piotrkowski, M.L. Harter, Cyclin-dependent kinases phosphorylate the adenovirus E1A protein, enhancing its ability to bind pRb and disrupt pRb-E2F complexes, *J. Virol.* 70 (1996) 2911–2921, <https://doi.org/10.1128/JVI.70.5.2911-2921.1996>.
- [35] Z.Q. Wu, X. Liu, Role for Plk1 phosphorylation of Hbo1 in regulation of replication licensing, *Proc. Natl. Acad. Sci. U. S. A.* 105 (2008) 1919–1924, <https://doi.org/10.1073/pnas.0712063105>.
- [36] M.J. Fedor, E. Daniell, Acetylation of histone-like proteins of adenovirus type 5, *J. Virol.* 35 (1980) 637–643, <https://doi.org/10.1128/JVI.35.3.637-643.1980>.
- [37] D.C. Avgousti, A.N. Della Fera, C.J. Otter, C. Herrmann, N.J. Pancholi, M.D. Weitzman, Adenovirus core protein VII downregulates the DNA damage response on the host genome, *J. Virol.* 91 (2017), <https://doi.org/10.1128/JVI.01089-17>.
- [38] J.S. Johnson, Y.N. Osheim, Y. Xue, M.R. Emanuel, P.W. Lewis, A. Bankovich, A.L. Beyer, D.A. Engel, Adenovirus protein VII condenses DNA, represses transcription, and associates with transcriptional activator E1A, *J. Virol.* 78 (2004) 6459–6468, <https://doi.org/10.1128/JVI.78.12.6459-6468.2004>.
- [39] P. Ostapchuk, M. Suomalainen, Y. Zheng, K. Boucke, U.F. Greber, P. Hearing, The adenovirus major core protein VII is dispensable for virion assembly but is essential for lytic infection, *PLoS Pathog.* 13 (2017) e1006455, <https://doi.org/10.1371/journal.ppat.1006455>.
- [40] J. Chen, N. Morral, D.A. Engel, Transcription releases protein VII from adenovirus chromatin, *Virology* 369 (2007) 411–422, <https://doi.org/10.1016/j.virol.2007.08.012>.

- [41] S. Baluchamy, H.N. Rajabi, R. Thimmapaya, A. Navaraj, B. Thimmapaya, Repression of c-Myc and inhibition of G1 exit in cells conditionally overexpressing p300 that is not dependent on its histone acetyltransferase activity, *Proc. Natl. Acad. Sci. U. S. A.* 100 (2003) 9524–9529, <https://doi.org/10.1073/pnas.1633700100>.
- [42] E. Harlow, B.R. Franza Jr., C. Schley, Monoclonal antibodies specific for adenovirus early region 1A proteins: extensive heterogeneity in early region 1A products, *J. Virol.* 55 (1985) 533–546.
- [43] N.C. Reich, P. Sarnow, E. Duprey, A.J. Levine, Monoclonal antibodies which recognize native and denatured forms of the adenovirus DNA-binding protein, *Virology* 128 (1983) 480–484.
- [44] M.M. Huang, P. Hearing, The adenovirus early region 4 open reading frame 6/7 protein regulates the DNA binding activity of the cellular transcription factor, E2F, through a direct complex, *Genes Dev.* 3 (1989) 1699–1710.
- [45] N. Jones, T. Shenk, Isolation of deletion and substitution mutants of adenovirus type 5, *Cell* 13 (1978) 181–188, [https://doi.org/10.1016/0092-8674\(78\)90148-4](https://doi.org/10.1016/0092-8674(78)90148-4).
- [46] S. Radko, M. Koleva, K.M. James, R. Jung, J.S. Mymryk, P. Pelka, Adenovirus E1A targets the DREF nuclear factor to regulate virus gene expression, DNA replication, and growth, *J. Virol.* 88 (2014) 13469–13481, <https://doi.org/10.1128/JVI.02538-14>.
- [47] R. Costa, N. Akkerman, D. Graves, L. Crisostomo, S. Bachus, P. Pelka, Characterization of adenovirus 5 E1A exon 1 deletion mutants in the viral replicative cycle, *Viruses* 12 (2020), <https://doi.org/10.3390/v12020213>.
- [48] A.M. Soriano, L. Crisostomo, M. Mendez, D. Graves, J.R. Frost, O. Olanubi, P.F. Whyte, P. Hearing, P. Pelka, Adenovirus 5 E1A interacts with E4orf3 to regulate viral chromatin organization, *J. Virol.* 93 (2019), <https://doi.org/10.1128/JVI.00157-19>.
- [49] S. Bachus, N. Akkerman, L. Fulham, D. Graves, C. Stephanson, H. Memon, M.S. Miller, P. Pelka, Adenovirus 5 vectors expressing SARS-CoV-2 proteins, *mSphere* 7 (2022) e0099821, <https://doi.org/10.1128/msphere.00998-21>.